www.rericjournal.ait.ac.th

Numerical and Experimental Investigations of Lateral Cantilever Shaft Vibration of Passive-Pitch Vertical-Axis Ocean Current

R. Hantoro*[1], I.K.A.P Utama[+], A. Sulisetyono[+] and Erwandi[#]

Abstract – *Simulation and experiment of lateral shaft vibration of passive variable-pitch vertical-axis ocean current turbine have been performed. A cantilever type of shaft has been used and modeled using finite element method, and simulated using consistent mass matrix to obtain the vibration characteristics and responses. Variations of incoming fluid velocity and the corresponding rpm were used to identify the pattern of lateral displacement responses. Analysis of displacement responses at all nodes in x and y-direction at the same time was carried out, and confirmed with the presents mode shapes. The repeated pattern of periodic displacement responses due to the functions of force acting on the foils was identified. Correlation of critical azimuth position of the foils and displacement responses was presented. Experiment was conducted as validation of the simulation results at a node of the finite element model. Periodic pattern responses resulted from simulation and experiment at the validated node shows the suitability with average error value for all variations were 11.6% in x-direction and 12.3% in y-direction.*

Keywords – Cantilever, finite-element, lateral vibration, passive variable-pitch, vertical-axis.

1. INTRODUCTION

Research on the effect of fluctuations of the force on the output power generated by energy conversion system from renewable energy sources (wind, ocean currents) has become a serious concern among researchers [1],[2]. In the case of ocean current turbine system, the force of the fluid causes structure to rotate and change its orientation to the incoming fluid flow. Force fluctuations which follow the turbine during rotation become potency of vibrations of the turbine shaft. For dynamic response analysis, a linearized finite element model was employed to establish a control scheme for rotor systems [3]. The finite element method was also applied to a complex rotor system to evaluate its vibration response due to fluid forces [4], and gyroscopic moments [5]. General purpose finite element codes [6] were adapted to simulate the dynamics of some complex rotor systems.

This paper discussed the characteristics of lateral vibration on the main shaft of vertical-axis ocean current turbine with the use of passive variable-pitch. A cantilever type of shaft was used and modeled using finite element method. Simulation was carried out using consistent mass matrix in the Matlab package to obtain the natural frequencies, mode shapes and deflection of vibration response. Fourier force function used in the simulation was taken from force fluctuations data obtained at previous CFD simulation [7], [8].

Test was conducted as validation of the simulation results at a node of the finite element model.

2. VIBRATIONS MODELING USING FINITE ELEMENT AND CONSISTENT MASS MATRIX

Although early dynamic models of rotor systems were formulated either analytically [9] or using transfer matrix approach [10], the potential of the powerful finite element technique was recognized at a very early stage [11]. In general, a structure is analyzed as a system of continuous or discrete systems (lumped system). A uniform structure like rod can be more appropriate if treated as a continuous system. Finite element method in fact can be called a combination of two methods, namely the continuous and discrete elements in the level of general coordinates.

In this study, the vertical axis turbine is modeled as a system consisting of the shaft which is divided into 10 elements. Three foils as producer of excitation force rests at two points on the shaft (node-3 and node-10), as shown in Figure 1. With the total length of 1400 mm, each element has length of 140 mm. Parameters of Cantilever shaft turbine used in simulation and experiments are:

Table 1. Material specifications.

- shaft material	:	SS304
- modulus elasticity (E)	:	200 GPa
- shear modulus (G)	:	86 GPa
- shaft dimension	:	Length 1400mm, diameter 44.5 mm
- density	:	8000 kg/m^3

*Post-Graduate Program, Faculty of Marine Technology, Kampus ITS Sukolilo Surabaya, Indonesia, 60111.

[+] Department of Naval Architecture and Shipbuilding Engineering Kampus ITS Sukolilo Surabaya, Indonesia, 60111.

[#] BPPT-LHI (Indonesian Hydrodynamic Laboratory) Kampus ITS Sukolilo Surabaya, Indonesia, 60111.

[1]Corresponding author; Tel: + 6231 5947188, Fax: +6231 5923626.
Email: hantoro@ep.its.ac.id.

The element stiffness matrix can be developed using basic strength of materials techniques to analyze the forces required to displace each degree of freedom a unit value in the positive direction. Using the degrees of freedom of element stiffness matrix results in the following element stiffness matrix:

$$K_{e;,i} = E_i I_i \begin{bmatrix} \frac{12}{l_i^3} & \frac{6}{l_i^2} & \frac{-12}{l_i^3} & \frac{6}{l_i^2} \\ \frac{6}{l_i^2} & \frac{4}{l_i} & \frac{-6}{l_i^2} & \frac{2}{l_i} \\ \frac{-12}{l_i^3} & \frac{-6}{l_i^2} & \frac{12}{l_i^3} & \frac{-6}{l_i^2} \\ \frac{6}{l_i^2} & \frac{2}{l_i} & \frac{-6}{l_i^2} & \frac{4}{l_i} \end{bmatrix} \quad (1)$$

Cantilever beam with two element model with one end not allowed to move is necessary to eliminate the degree of freedom. To eliminate the constrained degrees of freedom, the rows and columns which correspond to the constrained global degrees of freedom were eliminated, reducing the global stiffness matrix to a 4x4 matrix, resulting as in Equation 2.

$$K_g = \begin{bmatrix} \left(\frac{12E_1I_1}{l_1^3} + \frac{12E_2I_2}{l_1^3}\right) & \left(\frac{-6E_1I_1}{l_1^2} + \frac{6E_2I_2}{l_1^2}\right) & \frac{-12E_2I_2}{l_2^3} & \frac{6E_2I_2}{l_1^2} \\ \left(\frac{-6E_1I_2}{l_1^2} + \frac{6E_2I_2}{l_2^2}\right) & \left(\frac{4E_1I_1}{l_1^2} + \frac{4E_2I_2}{l_2^2}\right) & \frac{-6E_2I_2}{l_2^2} & \frac{2E_2I_2}{l_2} \\ \frac{-12E_2I_2}{l_2^3} & \frac{-6E_2I_2}{l_2^2} & \frac{12E_2I_2}{l_2^3} & \frac{-6E_2I_2}{l_2^2} \\ \frac{6E_2I_2}{l_2^2} & \frac{2E_2I_2}{l_2^2} & \frac{-6E_2I_2}{l_2^2} & \frac{4E_2I_2}{l_2} \end{bmatrix} \quad (2)$$

The same method can be performed on the number of element more than two with considering of the computing capability to perform high-order matrix operations. For a beam which is modeled with finite element method there are several method to form the mass matrix, namely: (a) lumped mass for the translation, (b) lumped mass for the translation and rotation, and (c) consistent mass - distributed mass effects. The parameters of mass and inertial mass matrix element connecting rods in the inertial load point to point and given the acceleration in the diagonal matrix. Equation 3 shows the lumped mass matrix (LM), including translation and rotation,

$$\begin{bmatrix} \left(\frac{ml}{2}\right) & 0 & 0 & 0 \\ 0 & \left(\frac{ml^3}{24} + \frac{mlI_y}{2A}\right) & 0 & 0 \\ 0 & 0 & \left(\frac{ml}{2}\right) & 0 \\ 0 & 0 & 0 & \left(\frac{ml^3}{24} + \frac{mlI_y}{2A}\right) \end{bmatrix} \quad (3)$$

Lumped mass formulations were state of the art in structural dynamics until Archer's classic paper [12] introduced the consistent mass matrix in 1963. Consistent mass (CM) Matrix for a beam element is,

$$m_{e;,i} = \frac{ml}{420} \begin{bmatrix} 156 & 22l & 54 & -13l \\ 22l & 4l^2 & 13l & -3l^2 \\ 54 & 13l & 156 & -22l \\ -13l & -3l^2 & -22l & 4l^2 \end{bmatrix} \quad (4)$$

With the same method to obtain the matrix $\mathbf{k_g}$ in Equations 1 and 2, the matrix CM for two elements $\mathbf{m_g}$ become,

$$m_g = \frac{1}{420} \begin{bmatrix} 312ml & 0 & 54ml & -13ml^2 \\ 0 & 8ml^3 & 13ml^2 & -3ml^3 \\ 54ml & 13ml^2 & 156ml & -22ml^2 \\ -13ml^2 & -3ml^3 & -22ml^2 & 4ml^3 \end{bmatrix} \quad (5)$$

With the acquisition of $\mathbf{m_g}$ and $\mathbf{k_g}$ then the eigenvalue problem for homogeneous equations of motion can be written as,

$$m_g \ddot{z} + k_g z = [0] \quad (6)$$

It is not obvious to weather the lumped mass matrices or consistent mass matrices yield more accurate result for general dynamic response problem [13]. The lumped mass matrices are approximate in the sense that they do not consider the dynamic coupling present between the various displacement degrees of freedom of the element. However, since the lumped mass matrices are diagonal, they required less storage space during computation. On the other hand, the consistent mass matrices are not diagonal and hence required more storage space. They too are approximate in the sense that the shape functions, which are derived using static displacement patterns, are used even for the solution of dynamics problems.

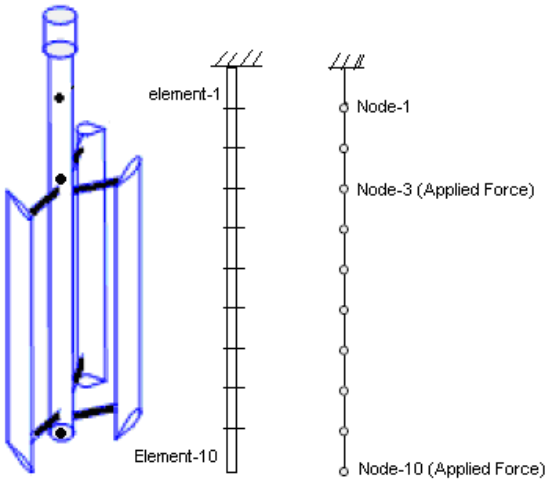

Fig. 1. Finite element model of vertical-axis turbine.

3. FOURIER FORCE FUNCTION MODELING

Equations obtained by Fourier-force function are used to obtain the vibration response respect to time and the external forces acting on the shaft. It is obtained by making Equation 6 become,

$$[m_g k_g][\bar{z}] = [\bar{F}] \quad (7)$$

and all nodes in the deviation of z is,

$$[\bar{z}] = [m_g k_g]^{-1}[\bar{F}] \quad (8)$$

CFD simulation performed on previous research by Hantoro *et al.* [7] have resulted the pattern of force fluctuations in variations of flow velocity and rotation speed of turbine. Variations that are performed in the CFD simulations are as follows:

Force fluctuation patterns appear in a full rotation at all variations classified in two directions as defined in Figure 2. Simulation of lateral vibration on the main shaft for every variation was performed in two directions, namely in x and y-direction. Force in x-direction is the force acting on a rotating turbine in the same direction with the incoming fluid flow, while the y-direction is for the force that is perpendicular to the incoming fluid flow.

The resulted force fluctuations of turbine for all variations which are acting on the shaft provides periodic pattern as shown in Figure 3.

Fourier force function modeling performed by taking a period (T) of fluctuation patterns. Results of modeling achieve agreement to fit after the 6th-order iterations. Plots of Fourier force function fluctuations performed with Matlab provides good agreement compared with the results of CFD data simulation. Figure 4 shows an example of the suitability at Var-2 variation.

Table 2. Towing tank variations test

Variation	U (m/s)	RPM
Var-1	0.6	28
Var-2	0.8	37
Var-3	1	45

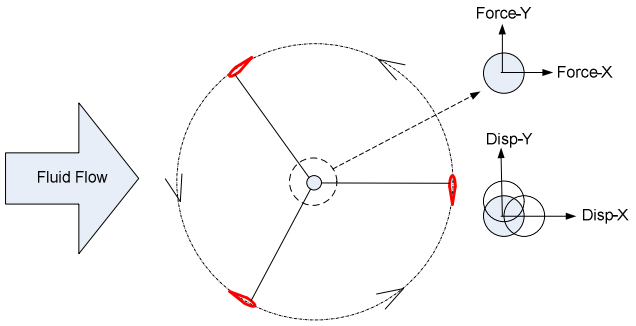

Fig. 2. Definition of the lateral direction of the force and the vibration on the main shaft of turbine.

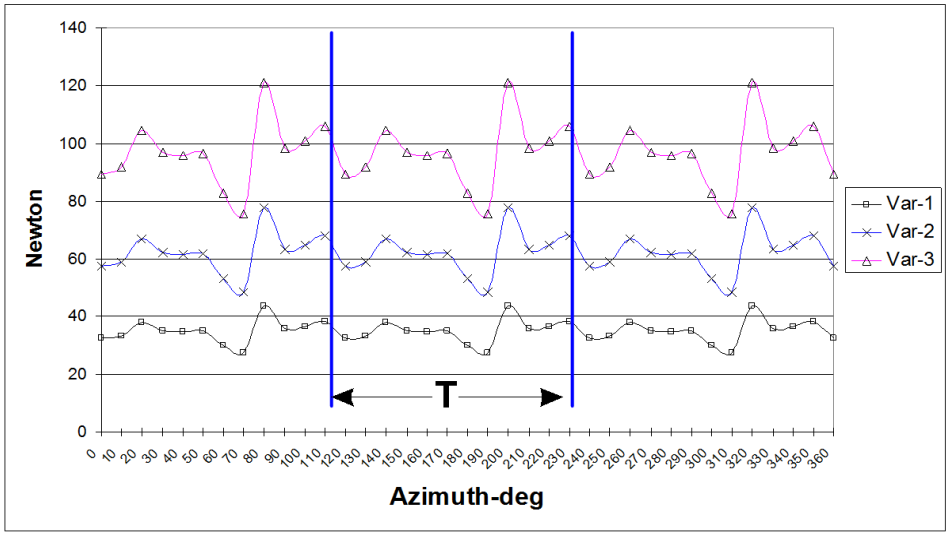

(a)

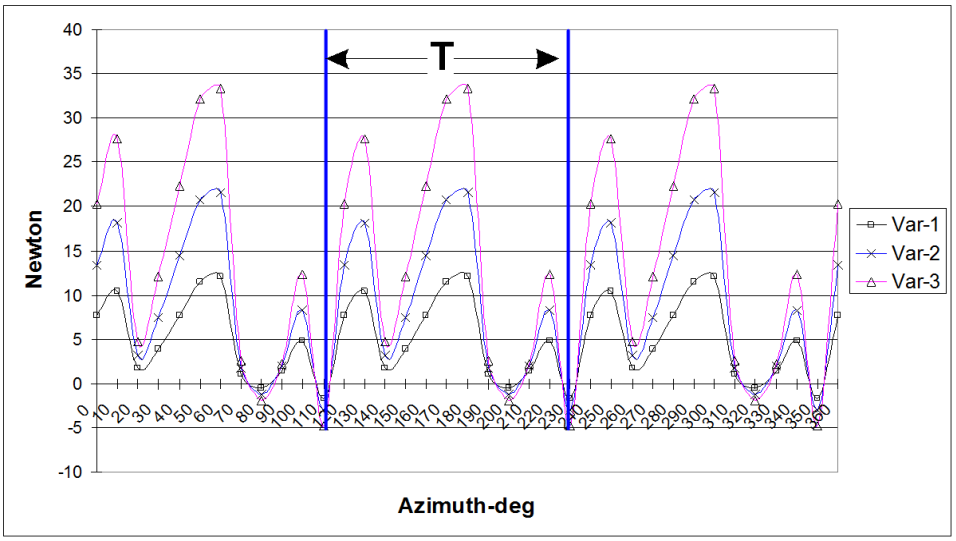

(b)

Fig. 3. Fluctuation pattern of the force at all variations, (a) x-direction, (b) y-direction.

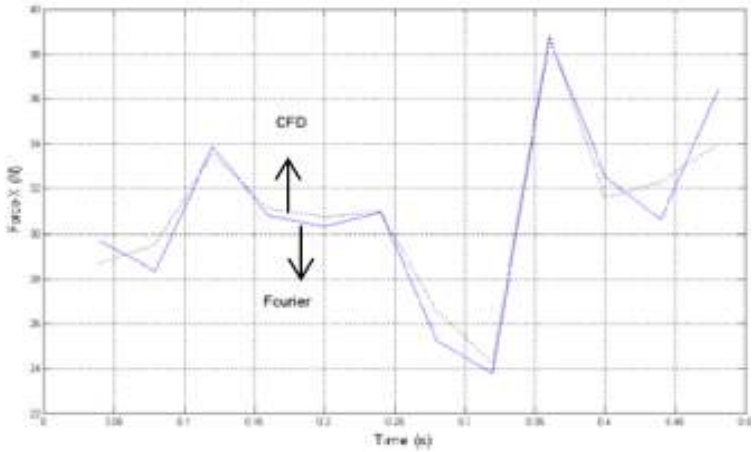

(a)

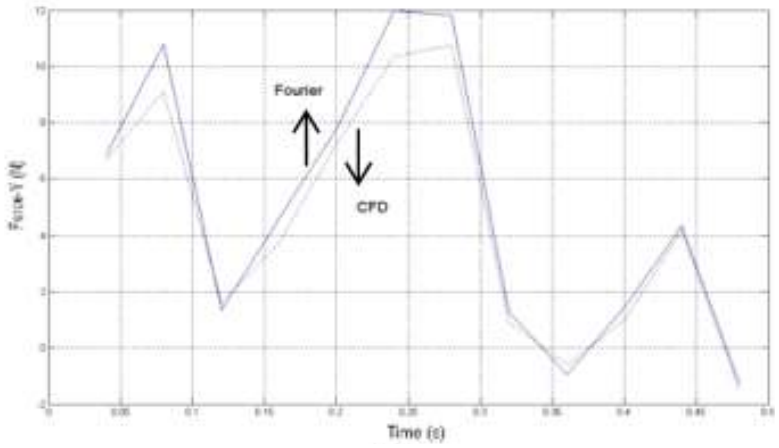

(b)

Fig. 4. The suitability of the force fluctuation pattern at Var-2 variations, (a) x-direction, (b) y- direction.

4. TESTING OF VIBRATION DISPLACEMENT

Experiments included the manufacture and testing of the work piece was carried out at the towing tank facility at Hydrodynamics Laboratory, Faculty of Marine Technology ITS, with specifications: 50 meters length, 3 meters wide, and 2 meters deep.

The foil chord was set at 100 millimeters, with span of 1000 mm giving aspect ratio of 10, and 500 mm arm to the shaft. The turbine was designed with three foils. The NACA 0018 profile was chosen as the foil section with data from [14]. This section is commonly used for Darrieus turbines. Its relatively high thickness to chord ratio gives it good strength in bending. The radial arms of the turbine were made from high strength aluminum. Turbine shaft used cantilever type with one end fixed by the bearing and the other end free (overhanging) as shown in Figure 6.

Data collection was conducted with the same variation as mention in Table 1. The use of passive variable-pitch allowed foil to change its relative position to the arm, where the position of the foil are given the freedom to move within the interval -10^0 to 10^0, as shown in Figure 7.

Magnetic probe sensor (eddy currents) is placed on node-1 in the x and y-direction with a distance of 140 mm from the bearing in order to obtain displacement data (Figure 8). Data collection was performed after towing tank carriage speed has stable with time sampling of 0.001 second.

Fig. 5. Towing tank facility at FTK ITS.

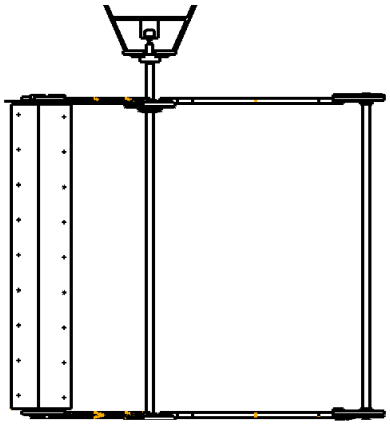

Fig. 6. Vertical-axis turbine with three straight foils.

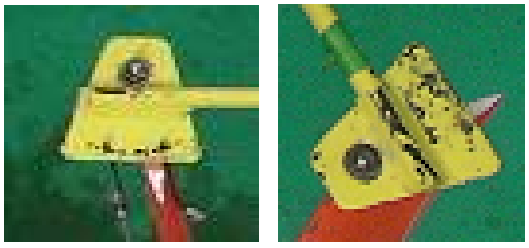

Fig. 7. Passive variable-pitch position relative to arm.

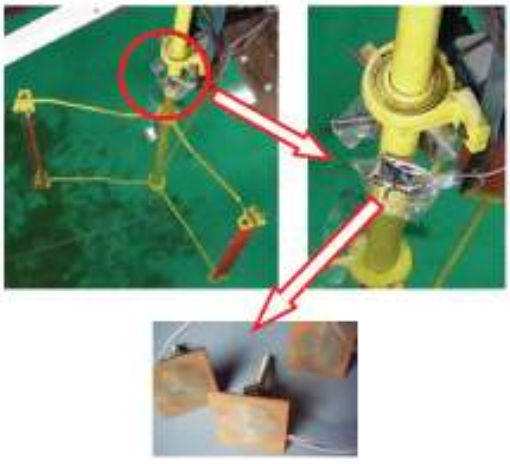

Fig. 8. Installation of Eddy current sensors to the turbine shaft.

4. RESULTS AND DISCUSSION

The natural frequency (**ωn**) was obtained by solving the roots of the determinant of the equations of motion using,

$$[m_g k_g][z] = [0] \quad (9)$$

$$\omega_n = \det[m_g k_g] \quad (10)$$

Coupling between elements gives the degrees of freedom two times the number of elements, resulting 20 varieties of natural frequency as shown in Figure 9 and Table 3.

Resulted displacement from simulation at all nodes at the same time indicating the possibility of mode shape

occurrence. Figure 10 shows the displacement at all nodes in x-direction at Var-2 for $t_{i=2}$, $t_{i=8}$, and $t_{i=36}$ (Figures 10a-10c). Similar mode of displacement at all node was presented for all variations in x and y-direction, and these modes recognized to be agreed to the 20th mode shape resulted from simulation (Figure 10d). Changes in inter-elements in the node-9 to give significant difference when compared to the other nodes. This indicates that the use of the cantilever shaft for vertical-axis ocean current turbine give potential problems on the tip of shaft. It is obvious due to half of the force received on turbine concentrated at cantilever tip.

Deflection at node-1 in a single rotation at all variations in x and y-direction shown in Figures 11 to 13. Vibration response generated in the simulation and testing in all variations give a periodic pattern follows the force pattern on the turbine shaft.

Table 3. Natural frequency of turbine shaft.

Mode	ω_n (Hz)	Mode	ω_n (Hz)
1	1	11	244
2	4	12	295
3	12	13	357
4	24	14	431
5	40	15	518
6	61	16	619
7	85	17	735
8	114	18	858
9	147	19	966
10	183	20	1210

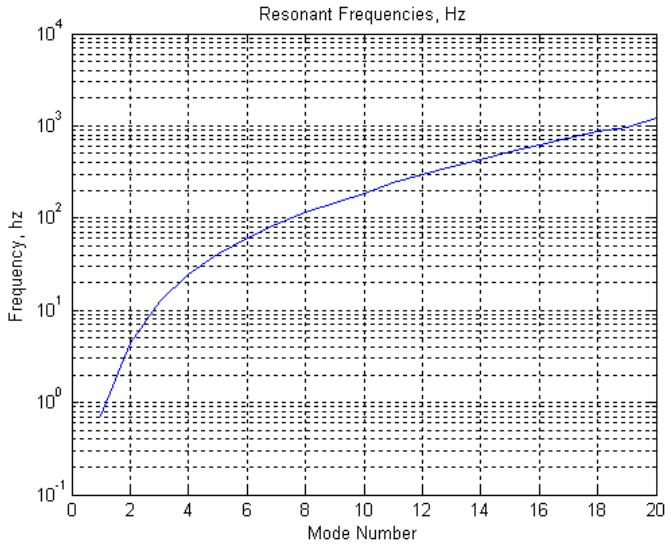

Fig. 9. Natural frequency of turbine shaft.

Responses of displacement appearing in x and y-direction are always positive. According to the definition of the direction of displacement which has been described previously, the position displacement is always in the region of x + and y +. Displacement at this area generated by the excitation force resulted from interaction between the incoming fluid and foils according to the position at the azimuth as the turbine rotates.

The highest deflection occurs at each variation according to the azimuth position (0^{0}-$360^{0)}$ of the turbine shown in Table 4. The increase in turbine rotation speed is generally deliver enhanced value of the lateral deviation in x and y-direction. However, the maximum deviation is not always occur at the same azimuth position despite the azimuth angle intervals are repeated consistently in value close or equal to 120^{0}.

The average error between the simulation and measurement at each of variation are given in Table 5. Greater average error resulted from experiment compared to simulation results. The average value of the resulting error for all variations in x-direction is 11.6%, whereas for y-direction is 12.3%.

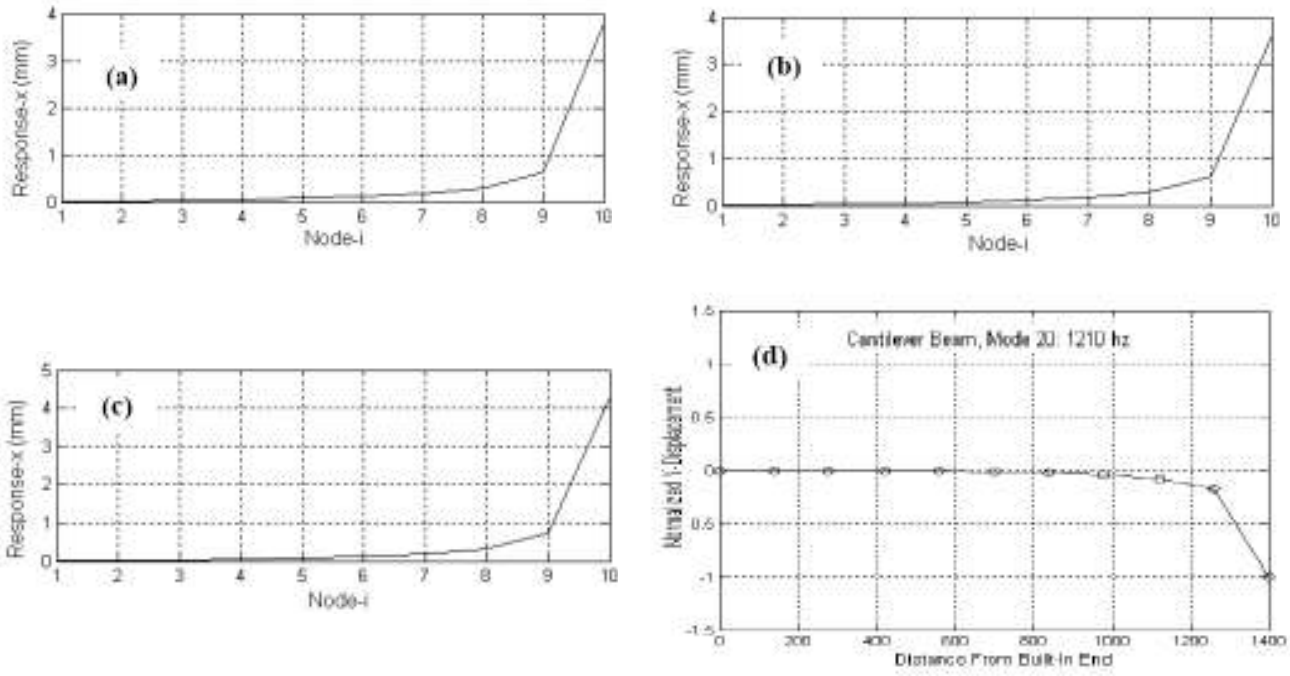

Fig. 10. Displacement all nodes at, (a) $t_{i=2}$, (b) $t_{i=8}$, (c) $t_{i=36}$, (d) 20th mode shape.

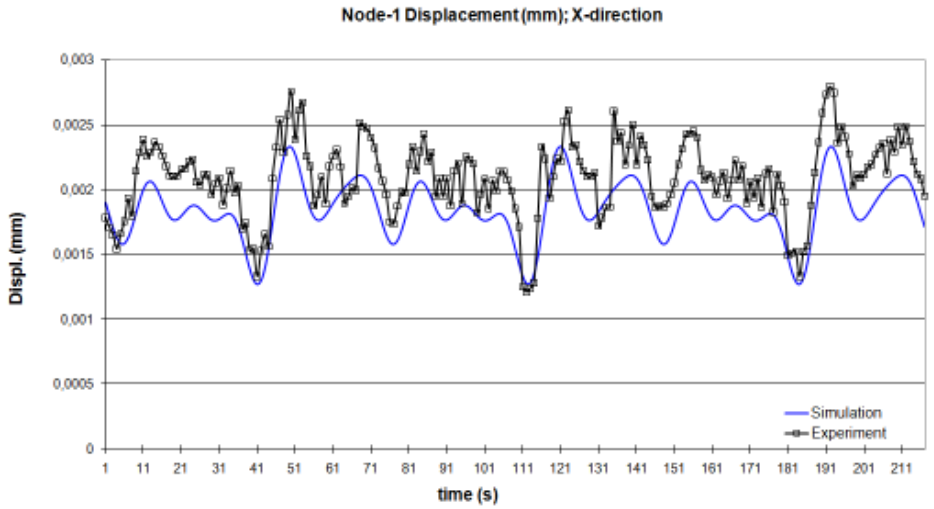

(a)

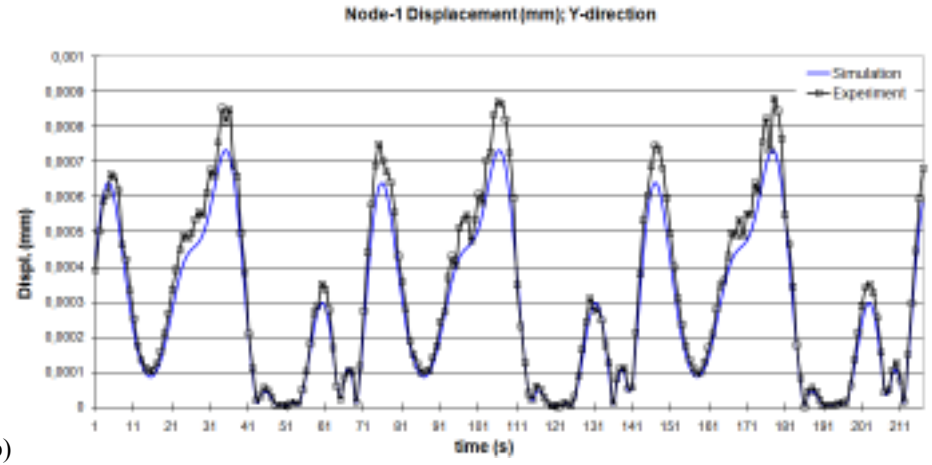

(b)

Fig. 11. Responses at node-1 at Var-1, (a) x-direction, (b) y-direction.

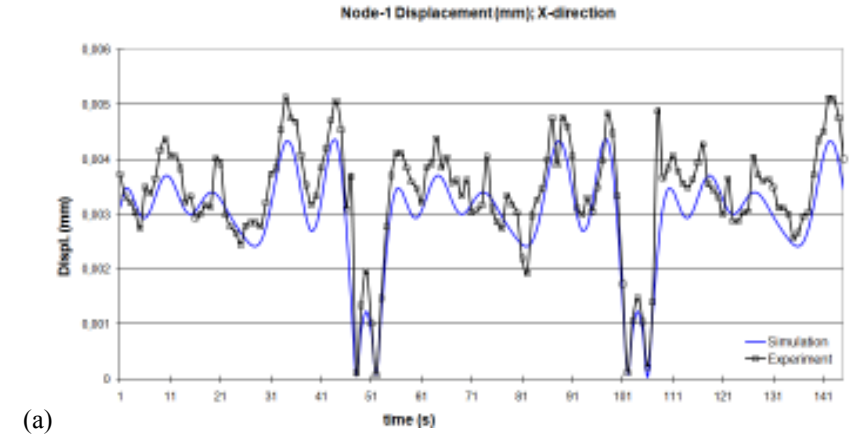

(a)

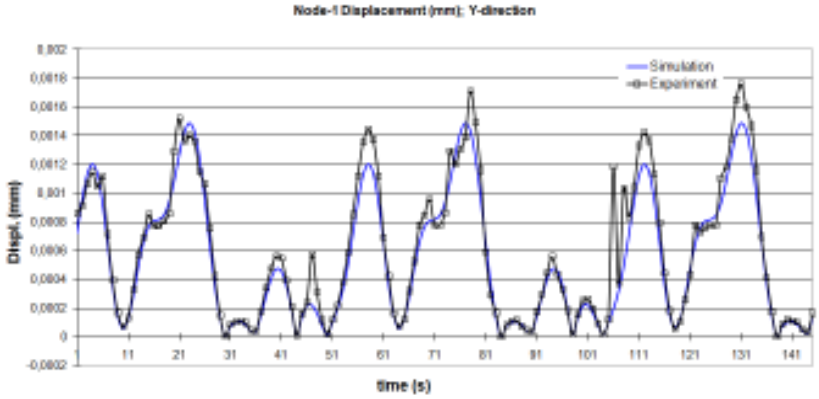

(b)

Fig. 12. Responses at node-1 at Var-2, (a) x-direction, (b) y-direction.

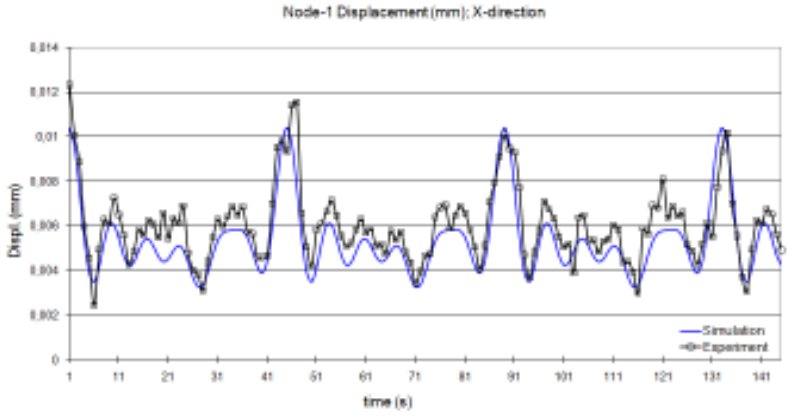

(a)

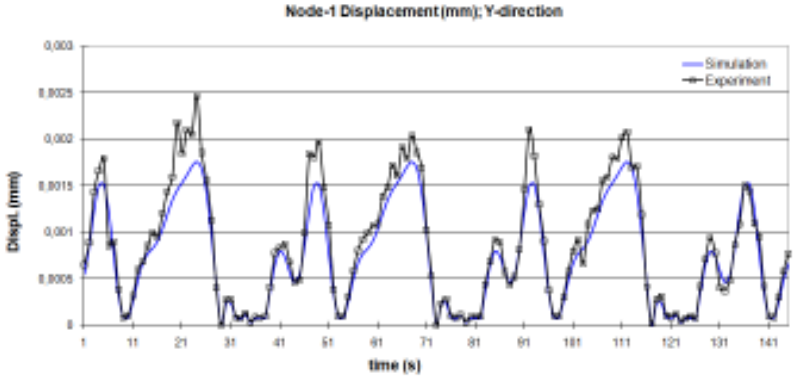

(b)

Fig. 13. Responses at node-1 at Var-3, (a) x-direction, (b) y-direction.

Table 4. Position of azimuth of the highest displacement.

U (m/s)	Direction	Azimuth (degree)
0.6	x	80^0, 200^0, 320^0
	y	60^0, 180^0, 300^0
0.8	x	110^0, 230^0, 350^0
	y	50^0, 190^0, 320^0
1	x	110^0, 220^0, 330^0
	y	50^0, 160^0, 280^0

Table 5. Average error for variations

U (m/s)	Average Error (%) x-direction	Average Error (%) y-direction
0.6	13.4	13.3
0.8	11.4	11
1	12.4	13.8

5. CONCLUSION

Simulation and testing of lateral vibration of passive variable-pitch vertical-axis ocean current turbine has been performed. Conclusions obtained from the research presented as follows:

Resulted displacement from simulation at all nodes at the same time indicating the present of the 20th of mode shape with natural frequency of 1230 Hz. Potential problems on the tip of shaft obviously due to half of the force of turbine received concentrated at cantilever tip.

The pattern of periodic displacement response repeat every 1/3 of turbine rotation and follows the functions of force acting on the foils. Critical position of foils for the occurrence of large displacement in x-direction is given when foil-1 positioned at the azimuth 50^0-80^0, foil-2 at 200^0-230^0, and foil-3 at 320^0-350^0. While on the y-direction is given when the foil-1 at azimuth positions 50^0-60^0, foil-2 at 160^0-190^0, and foil-3 at 280^0-320^0.

Comparison of simulation and test results at node-1 gave an average error value for all variations of 11.6% in x-direction and 12.3% in y-direction.

ACKNOWLEDGEMENT

The authors expresses their gratitude to DP2M Dikti and LPPM ITS for funding the research under research scheme known as Postgraduate Research Grand (HPTP) of the year 2009 and 2010.

The authors also thank the technicians at the ITS towing tank for their help in the experimental work.

REFERENCES

[1] Kiho, S., Shiono, M. and K. Suzuki, 1996. *The power generation from tidal currents by Darrieus turbine*. WRFC.

[2] Reuter, R.C. and M.H. Worstell, 1978. Torque ripple in a vertical axis wind turbine, Sandia Report SAND78-0577 l Unlimited Release UC-60.

[3] Firoozian, R. and R. Stanway, 1988. Modeling and control of turbomachinery vibrations. *Journal of Vibration and Acoustics, Stress, and Reliability in Design* 110: 521-527.

[4] Diewald, W. and R. Nordmann, 1989. Dynamic analysis of centrifugal pump rotors with fluid-mechanical interactions. *ASME Journal of Vibration and Acoustics, Stress, and Reliability in Design* 111: 370-378.

[5] Sakata, M., Kimura, K., Park S.K. and Ohnabe, H., 1989. Vibration of bladed flexible rotor due to gyroscopic moments. *Journal of Sound and Vibration* 131: 417-430.

[6] Rouch, K.E., Mcmaines, T.H., Stephenson, R.W. and Ermerick, M.F., 1989. Modeling of complex rotor systems by combining rotor and substructure models. In *4th International ANSYS Conference and Exhibition*, Part 2, 5.23-5.39.

[7] Hantoro. R., Utama. I.K.A.P., Erwandi, 2009. Unsteady load analysis on a vertical axis ocean current turbine. In the *11th International Conference on QIR (Quality In Research)*, 3-6 August, Indonesia University.

[8] Hantoro, R., Utama, I.K.A.P., Erwandi, Sulisetyono, A., 2009. Unsteady load and fluid-structure interaction of verical-axis ocean current turbine. *Journal of Mechanical Engineering, Petra University Surabaya* 11(1): 25-33.

[9] Dimentberg, F., 1961. *Flexural Vibrations of Rotating Shafts*. London: Butterworth.

[10] Black, H., 1974. A linearized model using transfer matrix to study the forced whirling of centrifugal pumps rotor systems *Journal of Engineering for Industry*.

[11] Ruhl, R.L. and J.F. Booker, 1972. A finite element model for distributed parameter turborotor systems. *ASME Journal of Engineering for Industry* 94, 126-132.

[12] Archer, J.S., 1963. Consistent mass matrix for distributed mass systems. Journal of the Structural Division, pp.161.

[13] Rao, S.S., 1995. *Mechanical Vibration*, 3rd Edition, Addison-Wesley Publishing Co., Inc.

[14] Sheldahl, R. and P. Klimas, 1981. Aerodynamic characteristics of seven symmetrical airfoil sections through 180-degree angle of attack for use in aerodynamic analysis of vertical axis wind turbines. Technical Report SAND80-2114, Sandia National Laboratories.